Supporting Information for

Linear $MgCp^*_2$ *vs.* Bent $CaCp^*_2$: London Dispersion, Ligand-Induced Charge Localizations and Pseudo-Pregostic C–H···Ca Interactions

Rumpa Pal,[a] Stefan Mebs,[b] Ming W. Shi,[c] Dylan Jayatilaka,[c] Joanna M. Krzeszczakowska,[d] Lorraine A. Malaspina,[a] Michal Wiecko,[e,f] Peter Luger,[e] Malte Hesse,[a] Yu-Sheng Chen,[g] Jens Beckmann,[a] Simon Grabowsky[a*]

[a] Universität Bremen, Institut für Anorganische Chemie und Kristallographie, Leobener Str. 3 and 7, 28359 Bremen, Germany

[b] Freie Universität Berlin, Institut für Experimentalphysik, Arnimallee 14, 14195 Berlin, Germany

[c] The University of Western Australia, School of Molecular Sciences, 35 Stirling Highway, Perth WA 6009, Australia

[d] University of Warsaw, Biological and Chemical Research Centre, Chemistry Department, Zwirki i Wigury 101, 02-089 Warsaw, Poland

[e] Freie Universität Berlin, Institut für Chemie und Biochemie, Anorganische Chemie, Fabeckstr. 36a, 14195 Berlin, Germany

[f] Current address: Bundesinstitut für Risikobewertung, Max-Dohrn-Straße 8-10, 10589 Berlin, Germany

[g] ChemMatCARS, Center for Advanced Radiation Sources, c/o Advanced Photon Source/ANL, The University of Chicago, 9700 South Cass Avenue, Bldg. 434D, Argonne, Illinois 60439, USA

* Correspondence to simon.grabowsky@uni-bremen.de

Contents

1) London dispersion and analysis of methyl…methyl interactions.

Table S1. Comparison of experimental and theoretical (B3LYP-D3/6-311++G(2d,2p)) geometrical parameters of $CaCp^*_2$ and $MgCp^*_2$. Geometrical parameters for the remaining model systems (Figure 2) as well as for Cp^- and Cp^{*-} and all electron-density parameters are derived from theory only.[%]

		C_r-C_r	Cr-C_{Me}	M-C_r	M-Cg	$C_{Me}\cdots C_{Me}$	$H_{Me}\cdots H_{Me}$	α[#]	β	γ
$CaCp^*_2$, bent	**d / angle**	1.422	1.504	2.617	2.320	min: 3.865	min: 2.446	155.1	32.6	1.7
						max: 6.111	max: 5.201			
	ρ(r)	1.97	1.67	0.20	N/A	N/A	min: 0.03			
	$\nabla^2\rho(r)$	-17.6	-13.2	2.8	N/A	N/A	min: 0.4			
$CaCp^*_2$, expt[§]	**d / angle**	1.419(1)	1.501(1)	2.633(8)	2.341(4)	min: 3.455(1)	min: 2.282	147.6(1)	19.3(1)	2.5(1)
						max: 6.323(1)	max: 6.196			
$CaCp^*_2$, linear	**d / angle**	1.424	1.506	2.642	2.348	5.207	4.010	179.9	36.0	2.5
	ρ(r)	1.96	1.66	0.19	N/A	N/A	N/A			
	$\nabla^2\rho(r)$	-17.5	-13.1	2.7	N/A	N/A	N/A			
$CaCp_2$	**d / angle**	1.416	N/A	2.639	2.349	N/A	N/A	179.9	35.9	N/A
	ρ(r)	1.99	N/A	0.18	N/A	N/A	N/A			
	$\nabla^2\rho(r)$	-18.1	N/A	2.7	N/A	N/A	N/A			
$MgCp^*_2$	**d / angle**	1.427	1.503	2.312	1.968	4.370	3.060	180.0	36.0	1.1
	ρ(r)	1.95	1.68	0.28	N/A	N/A	0.01			
	$\nabla^2\rho(r)$	-17.1	-13.3	2.4	N/A	N/A	0.1			
$MgCp^*_2$, expt										
Mol1, eclipsed	**d / angle**	1.427(2)	1.504(2)	2.308(6)	1.963(1)	4.019(2)	3.160	177.6(1)	8.1(1)	0.8(1)
Mol2, staggered	**d / angle**	1.425(2)	1.504(2)	2.304(6)	1.959(1)	4.339(2)	3.151	180.0[&]	36.0(1)	0.9(1)
$MgCp_2$	**d / angle**	1.419	N/A	2.336	2.001	N/A	N/A	179.9	36.0	N/A
	ρ(r)	1.97	N/A	0.20	N/A	N/A	N/A			
	$\nabla^2\rho(r)$	-17.8	N/A	3.6	N/A	N/A	N/A			
$CaCp^{*+}$	**d**	1.426	1.504	2.499	2.185	N/A	N/A	N/A	N/A	2.2
	ρ(r)	1.96	1.67	0.26	N/A	N/A	N/A			
	$\nabla^2\rho(r)$	-17.4	-13.2	3.3	N/A	N/A	N/A			
$CaCp^+$	**d**	1.418	N/A	2.520	2.213	N/A	N/A	N/A	N/A	N/A
	ρ(r)	1.98	N/A	0.25	N/A	N/A	N/A			
	$\nabla^2\rho(r)$	-18.1	N/A	3.2	N/A	N/A	N/A			
$MgCp^{*+}$	**d**	1.441	1.503	2.214	1.844	N/A	N/A	N/A	N/A	3.8
	ρ(r)	1.91	1.68	0.27	N/A	N/A	N/A			
	$\nabla^2\rho(r)$	-16.4	-13.3	4.8	N/A	N/A	N/A			
$MgCp^+$	**d**	1.429	N/A	2.221	1.859	N/A				
	ρ(r)	1.95	N/A	0.26	N/A	N/A				
	$\nabla^2\rho(r)$	-17.3	N/A	4.8	N/A	N/A				
Cp^{*-}	**d**	1.416	1.502	N/A	N/A	N/A				
	ρ(r)	1.99	1.67	N/A	N/A	N/A				
	$\nabla^2\rho(r)$	-18.0	-13.2	N/A	N/A	N/A				

Cp^-	**d**	1.413	N/A	N/A	N/A	N/A
	ρ(r)	1.99	N/A	N/A	N/A	N/A
	$\nabla^2\rho(r)$	-18.4	N/A	N/A	N/A	N/A

[%] Distances d in Å, angles α, β, γ (as defined in the inlet of the table) in °, electron density ρ at the bond critical points **r** in $eÅ^{-3}$, corresponding Laplacian values of the electron density in $eÅ^{-5}$. C_r…ring carbon atom; C_{Me}…methyl carbon atom; Cg…ring center of gravity. Except for the angle α and except for those entries where minimum and maximum values are given, all entries refer to averaged values. In nearly all cases, the sample standard deviations are smaller than the number of digits given in this table, so that we did not add them. [#]The definitions of the α,β,γ angles are as given in ref. 28 and in the inlet to the table. This scheme was reprinted with permission from ref. 28. Copyright (2003) American Chemical Society. [§]There are two symmetry-independent molecules in the asymmetric unit of $CaCp^*_2$. Only the molecule with no disorder in the five-membered ring was considered in this table, and only the major disorder component for the methyl groups. [&]There is no standard deviation for this angle, because only half a molecule is symmetry-independent and the other half is generated by crystallographic mirror symmetry.

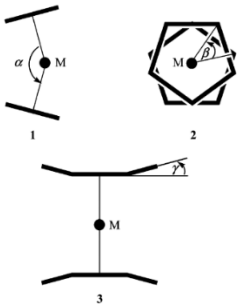

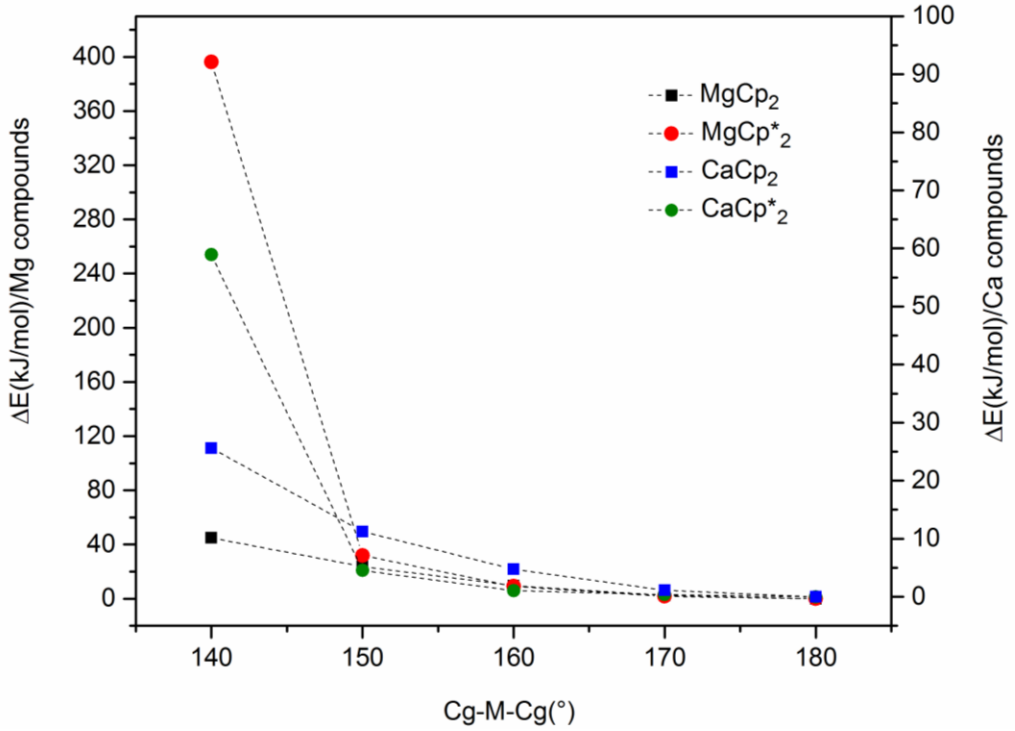

Figure S1. Relaxed PES scans at the B3LYP-D3/6-31G(d) level of theory. The energies given are relative to the linear geometries. Note that according to this level of theory, the linear geometry is the only minimum for all the four compounds, cf. Figure 3. However, the bending potentials for the Mg compounds are much steeper, and those for the Ca compounds are much flatter, which is indicated by the use of two different scaling of the ordinates (left ordinate for Mg compounds, right ordinate for Ca compounds).

Discussion on the effect of dispersion on the electron density:

In the main text, it is established that the B3LYP and B3LYP-D3 electron densities are identical. On the other hand, the MP2 calculations include both the effects of electron correlation and dispersion on the electron density. Therefore, the difference between the MP2 and B3LYP/B3LYP-D3 electron densities should show the regions in space which are responsible for the dispersion part of the methyl-methyl interactions (Figure 6 in the main text). Certainly, the major difference between the electron densities will not be dispersion, but insufficient treatment of the core region by DFT methods and different treatment of electron correlation between the methods. Dispersion effects cannot be separated from all other differences between MP2 and DFT (a corresponding difference plot between MP2 and HF showing pure electron correlation is shown in Figure S2 c). However, dispersion effects on the density can only occur inside these regions, not outside of them. At the contour level of ±0.009 au (Figure 6), the electron density isosurfaces occur rather close to the atoms (see also normalized difference density plots, Figure S3, and NCI difference plots, Figures S5 and S6).

This implies two points. First, the differences in dispersion (and any other difference between MP2 or B3LYP) occur near the atomic cores where the electron density is large. The center of the core electrons is shifted a little bit away from the original center due to the instantaneous dipole - induced dipole interactions. This small shift causes a dipole-dipole attraction or repulsion as a function of the distance between the two electron clouds of the cores. Second, in the region between the methyl groups where the reduced density gradient is large (NCI plots, Figure 5), there is only a very small difference between the MP2 and B3LYP electron densities, only visible at a contour of -10^{-6} a.u. (Figure S2 b). Hence, the dispersion interaction does not affect the electron density significantly in this region between the atoms. (See the table of contents graphic for a difference NCI plot between MP2 and HF calculation, depicting pure correlation beyond dispersion, contour level = ± 0.01 a.u. , blue = positive, red = negative, also Figure S6.)

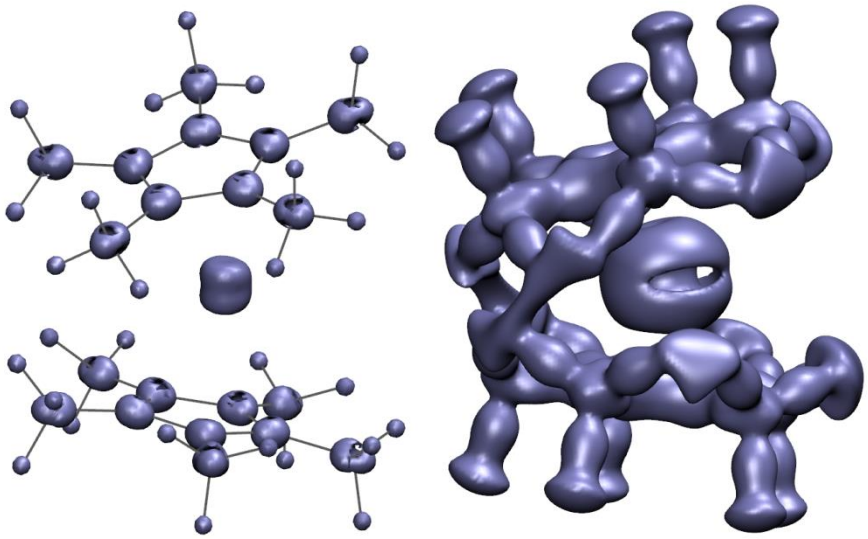

(a) (b)

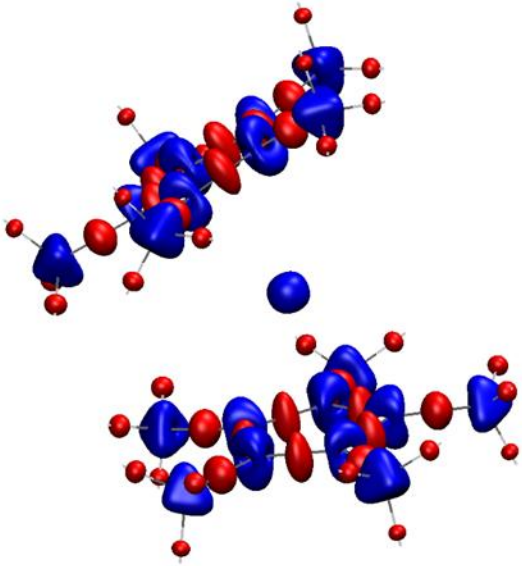

(c)

Figure S2. (a), (b) Differences of the MP2 and B3LYP electron densities for $CaCp^*_2$. Contour levels (a) -0.003 a.u. and (b) -10^{-6} a.u. (c) Difference of the MP2 and HF electron densities for $CaCp^*_2$. Contour levels $\pm$ 0.004 a.u., blue = positive, red = negative.

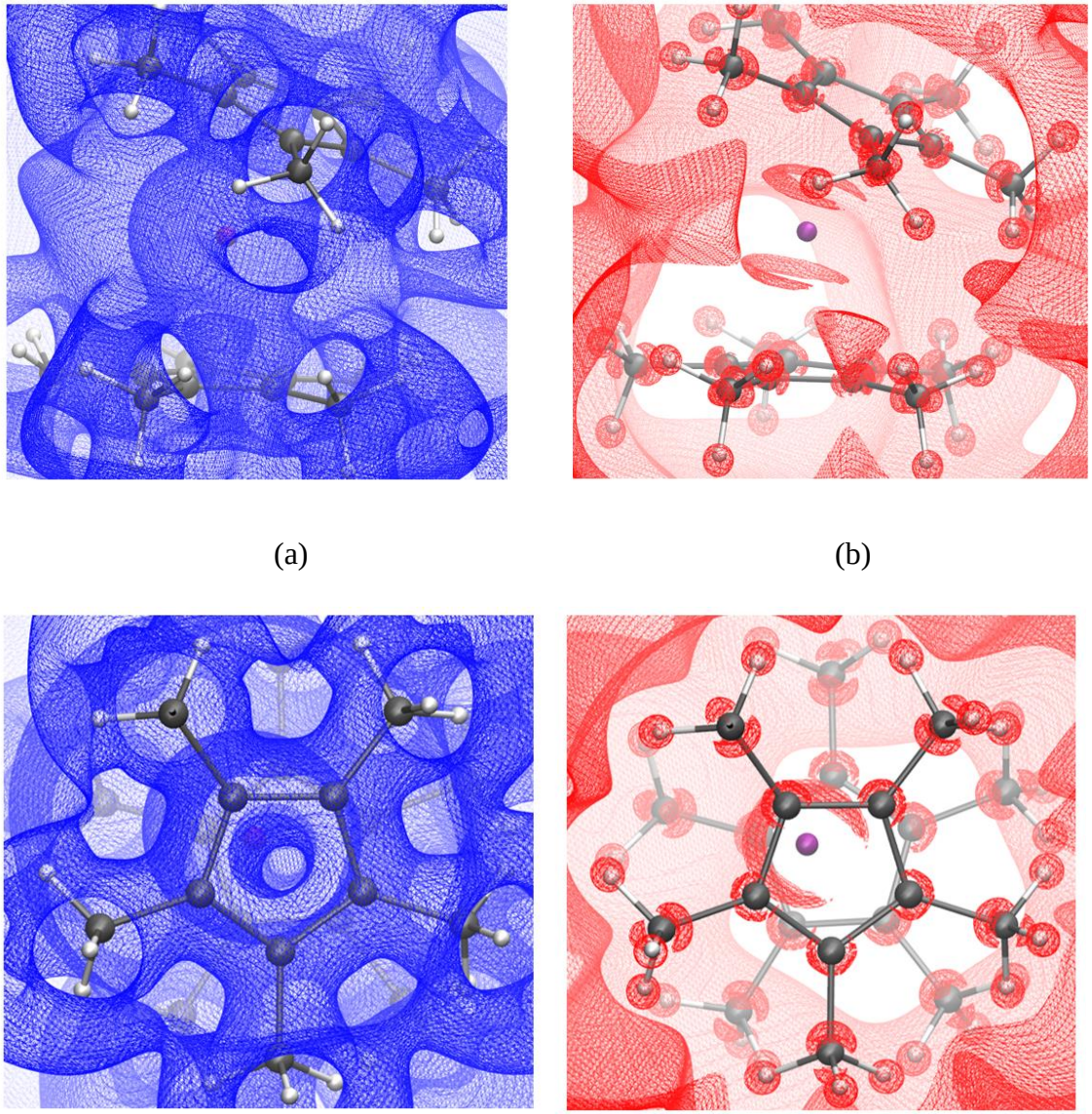

Figure S3. Normalized difference density plots for $CaCp^*_2$, (MP2 minus B3LYP) divided by B3LYP, in two different orientations. Blue = positive, red = negative. (a) and (c) isovalue = 0.02 a.u.; (b) and (d) isovalue = -0.02 a.u.

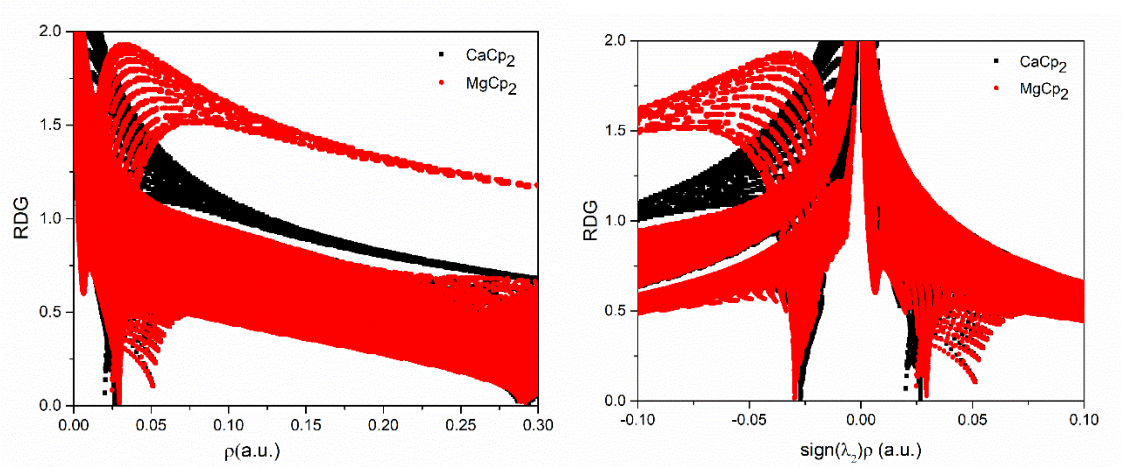

(a) (b)

Figure S4 (a), (b). Reduced density gradient of $CaCp_2$ and $MgCp_2$ at the B3LYP-D3/6-311++G(2d,2p) level of theory plotted against (a) the electron density, and (b) the electron density multiplied by the sign of the second Hessian eigenvalue.

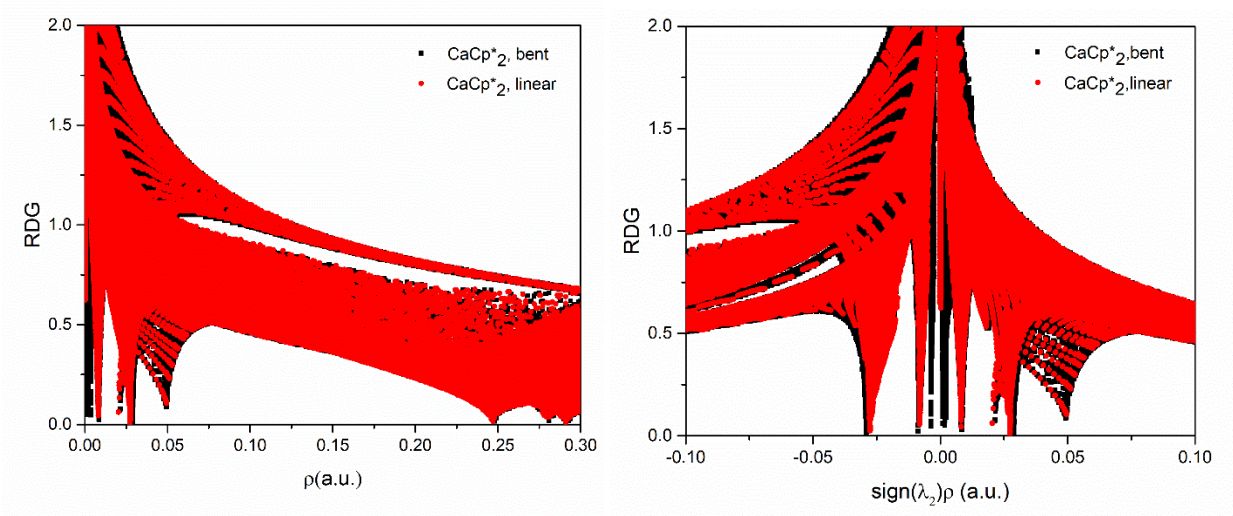

(c) (d)

Figure S4 (c), (d). Reduced density gradient of $CaCp^*_2$, bent, and $CaCp^*_2$, linear, at the B3LYP-D/6-311++G(2d,2p) level of theory plotted against (c) the electron density, and (d) the electron density multiplied by the sign of the second Hessian eigenvalue.

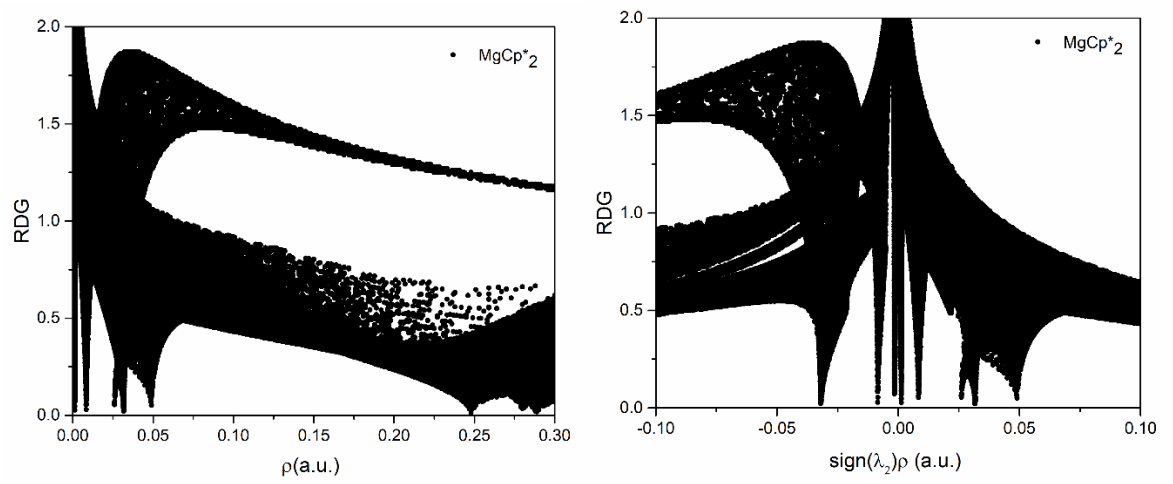

(e) (f)

Figure S4 (e), (f). Reduced density gradient of $MgCp^*_2$ at the B3LYP-D/6-311++G(2d,2p) level of theory plotted against (e) the electron density, and (f) the electron density multiplied by the sign of the second Hessian eigenvalue.

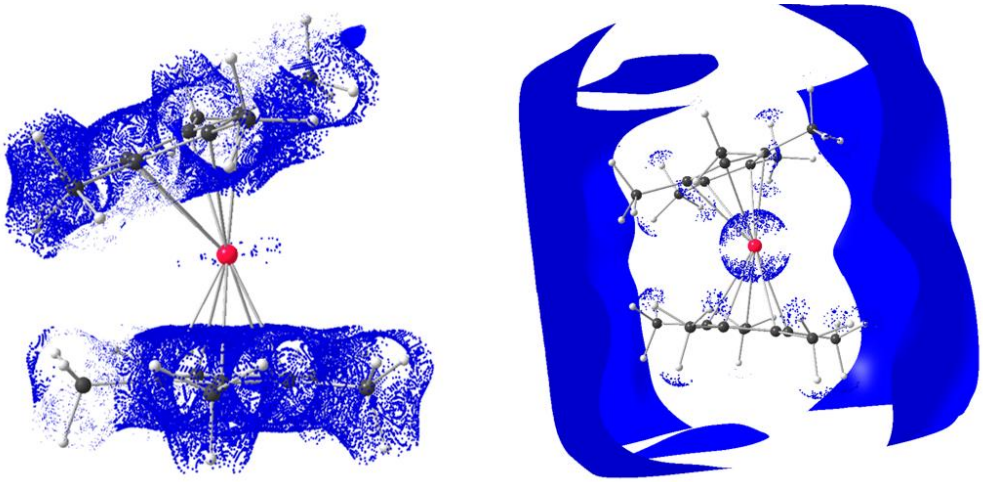

(a) (b)

Figure S5. NCI difference plots for $CaCp^*_2$, MP2 minus B3LYP. (a) RDG isovalue = 0.5; (b) RDG isovalue = -0.5.

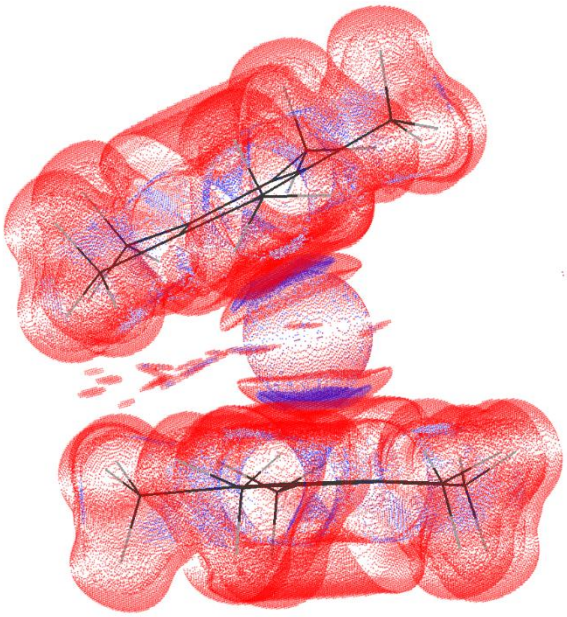

(i)

Figure S6. NCI difference plots for $CaCp^*_2$, MP2 minus HF. Contour level = ± 0.01 a.u. , blue = positive, red = negative.

2) Nature of the Metal Ion and the Metal…Cp* Bonding

In the following, the ELI-D and ED topologies are considered quantitatively, starting with the isolated rings: The average C_r–C_r (r = ring) distance is slightly longer in Cp^{*-} compared to Cp^-, 1.416 Å compared to 1.413 Å, but the ρ_{bcp} and $\nabla^2\rho_{bcp}$ values are similar in both systems (Table S1). In the ELI-D picture, there are more pronounced differences in these two ligands. The disynaptic $V_2(C_r,C_r)$ basin for Cp^{*-} carries an average population of 3.03 electrons (Table S2), compared to 2.88 electrons in the Cp^- ligand, which shows the stronger donor character of Cp^{*-} compared to Cp^-. Upon complex formation, the geometry and associated topological properties (Table 1, Table S1) show that the aromatic C_r–C_r bond length increases, 1.416 Å in free Cp^{*-} and 1.422 Å in $CaCp^*_2$, bent; corresponding ρ_{bcp} and $\nabla^2\rho_{bcp}$ values decrease, 1.99 e $Å^{-3}$ and -18.0 e $Å^{-5}$ in free Cp^{*-} and 1.97 e $Å^{-3}$ and -17.6 e $Å^{-5}$ in bent $CaCp^*_2$.

The electron population of the $V_2(M,C_r)$ basins in the complexes almost exclusively comes from the C–C bonds in the aromatic Cp^{*-} ligands, which decreases the populations of the newly formed $V_3(M,C_r,C_r)$ basins in all the metal complexes relative to free Cp^{*-} or Cp^-. For example, in $CaCp^{*+}$, the average electron population value in the $V_2(Ca,C_r)$ basin is 0.242e which is almost equal to the

decrease in the electron population value of $V_3(Ca,C_r,C_r)$ in the $CaCp^{*+}$ complex, 2.750e, compared to the $V_2(C_r,C_r)$ basin, 3.03e, in the gas-phase optimized structure of free Cp^{*-}. The topological analysis of the ELI-D shows that in $CaCp^{*+}$, the electrons in the $V_3(M,C_r,C_r)$ π-basins are more localized compared to the $V_2(Ca,C_r)$ σ-basin, as reflected in higher ELI-D value ($ELI\text{-}D_{max}$= 1.862, 1.361, respectively) and lower d_{max} value (0.115 and 0.826, respectively), (Table S2). Thus the former come close to the value for certainly quite localized $V_2(C_r,C_{Me})$ electrons, ($ELI\text{-}D_{max}$=1.999, d_{max} = 0.007).

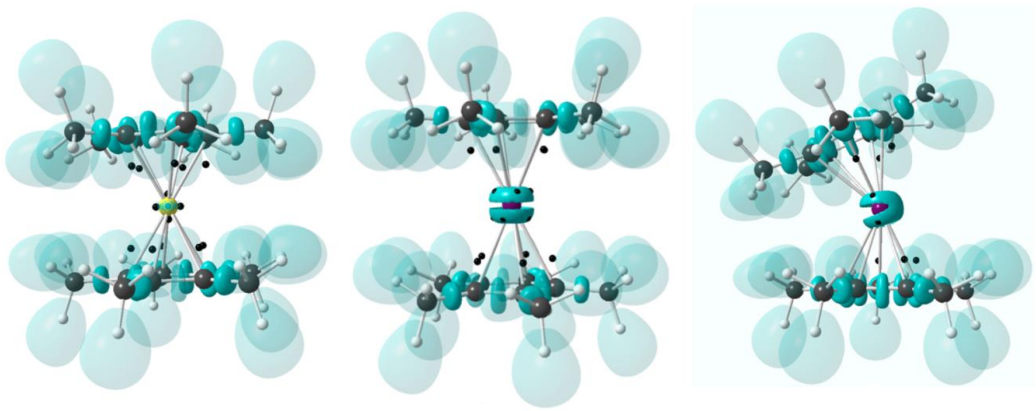

(a) (b) (c)

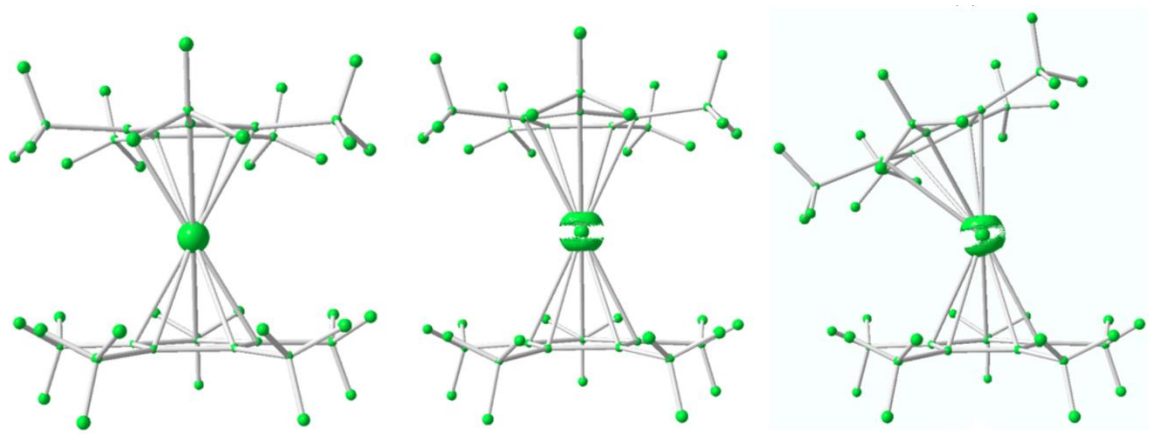

(d) (e) (f)

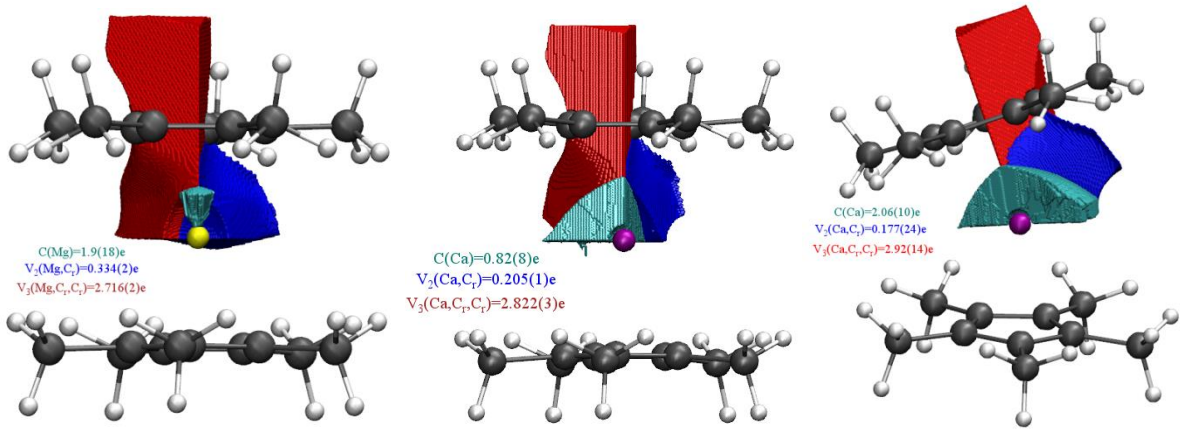

(g) (h) (i)

Figure S7. ELI-D localization-domain representation of (a) $MgCp^*_2$, (b) $CaCp^*_2$, linear, and (c) $CaCp^*_2$, bent, at an isovalue of 1.578. H atom domains are depicted in transparent modes. Black dots are attractors of ELI basins. (d), (e) and (f) are corresponding Laplacian plots with an isovalue of -3.78 au. (g), (h) and (i) are ELI-D basin representations (one representative basin per core or valence basin type) delineated with their zero-flux surfaces, or truncated at an electron-density isovalue of 0.001 au, and averaged over all basins per core or valence basin type. The basin populations are also cut at the same isovalue. Core basins [C(M)] are given in turquoise/ green, disynaptic valence basins [V(M,C_{ring})] in dark blue and trisynaptic valence basins [V(M,C_{ring},C_{ring})] in red. Values in brackets are the population standard deviations upon averaging.

Table S2. Topological and integrated ELI-D bond descriptors of free Cp^-, Cp^{*-} and all model systems (Figure 2). V_{001} and N_{001} are the volume and the electron population, respectively, cut at an outer electron-density isosurface of 0.001 au. μ_{max} is the ELI-D function value at the attractor of the basin. d_{max} is the distance of the attractor perpendicular to the linear bond axis. The values in brackets are the population standard deviations upon averaging if the deviations are significant.

Model	Basin	No.	V_{001}[Å^3]	N_{001}[e]	μ_{max}	d_{max} [Å]
Free Cp^-	V_2 (C_r,C_r)	5	9.980(3)	2.880(4)	1.859	0.065
Free Cp^{*-}	V_2 (C_r,C_r)	5	10.0(7)	3.03(6)	1.848(1)	0.070(2)
	V_2 (C_r,C_{Me})	5	3.020(4)	2.001	1.983(1)	0.004
$CaCp^+$	C (Ca)	5	0.64(7)	0.67(6)	1.598	0.304(2)
	C (Ca)	5	2.23(27)	0.97(11)	1.631	0.640
	V_2 (Ca,C_r)	5	1.175(61)	0.111(7)	1.337	0.836
	V_3 (Ca,C_r,C_r)	5	7.487(40)	2.756(6)	1.866	0.105

$CaCp^{*+}$	C (Ca)	5	0.66(5)	0.69(6)	1.596	0.304(4)
	C (Ca)	5	2.28(52)	0.96(22)	1.629	0.640
	V_2 (Ca,C_r)	5	1.806(3)	0.242(1)	1.361	0.826
	V_3 (Ca, C_r,C_r)	5	7.057(12)	2.750(4)	1.862	0.115
	V_2 (C_r,C_{Me})	5	3.003(3)	1.997(1)	1.999	0.007
$CaCp_2$, linear	C(Ca)	2	0.0717(8)	3.81(3)	1.5411	0.1640
	C(Ca)	10	1.1(1)	0.82(6)	1.611	0.361(4)
	V_3(Ca,C_r,C_r)	10	8.904(4)	2.8900(9)	1.856	0.089
$CaCp^*_2$, linear	C(Ca)	2	0.072(5)	3.77(40)	1.542	0.1640
	C(Ca)	10	1.11(11)	0.82(8)	1.610	0.35(1)
	V_2(Ca,C_r)	10	1.651(10)	0.205(1)	1.371	0.826
	V_3(Ca,C_r,C_r)	10	7.65(2)	2.822(3)	1.852	0.0979
	V_2(C_r,C_{Me})	10	2.995(2)	1.9913(4)	1.995	0.004
$CaCp^*_2$, bent	C(Ca)	4	2.79(19)	2.06(10)	1.609	0.26(5)
	V_2 (Ca,C_r)	6	1.37(17)	0.177(24)	1.370(2)	0.820
	V_3(Ca,C_r,C_r)	10	8.27(9)	2.92(14)	1.851	0.099(3)
	V_2(C_r,C_{Me})	10	2.99(1)	1.992(1)	1.995	0.002(1)
$MgCp^+$	C(Mg)	6	5.17(22)	1.31(23)	1.58007(8)	0.352(8)
	V_2 (Mg,C_r)	5	4.340(9)	0.3885(7)	1.3674(1)	0.3985(0)
	V_3 (Mg,C_r,C_r)	5	5.417(4)	2.515(1)	1.867	0.1085
$MgCp^{*+}$	C (Mg)	6	0.74(19)	1.31(25)	1.580	0.348(4)
	V_2 (Mg,C_r)	5	3.046(4)	2.0088(8)	2.00234(5)	0.0119(5)
	V_2 (C_r,C_{Me})	5	4.935(19)	0.509(1)	1.3909(1)	0.4230(5)
	V_3(Mg,C_r,C_r)	5	5.404(26)	2.521(9)	1.866	0.1101
$MgCp_2$	C(Mg)	7	0.5(3)	1.1(6)	1.5787(9)	0.3(6)
	V_2 (Mg,C_r)	10	1.49(1)	0.213(1)	1.3624(2)	0.8573
	V_3(Mg,C_r,C_r)	10	7.158(9)	2.703(2)	1.85112(4)	0.100
$MgCp^*_2$	C (Mg)	4	0.78(78)	1.9(18)	1.578(1)	0.349
	V_2 (Mg,C_r)	10	2.216(12)	0.334(2)	1.3886(3)	0.332(1)
	V_3 (Mg,C_r,C_r)	10	6.831(23)	2.716(2)	1.8454(1)	0.1096(4)
	V_2 (C_r,C_{Me})	10	3.010(3)	1.9940(4)	1.99708(4)	0.0002(5)

Table S3. NPA metal charges Q(M) in e and metal NAO Valence Populations for Ca and Mg in all model systems at B3LYP-D3 or B3LYP / 6-311++g(2d,2p) level. For Ca, 4s, 4p, 3d orbitals; for Mg, 3s, 3p, 3d orbitals.

	Q(M)	s	p_x	p_y	p_z	d_{xy}	d_{xz}	d_{yz}	d_{x2-y2}	d_{z2}
$CaCp^*_2$,bent	1.776	0.066	0.003	0.008	0.005	0.062	0.059	0.004	0.008	0.010
$CaCp^*_2$,linear	1.788	0.064	0.002	0.006	0.010	0.060	0.062	0.001	0.006	0.002
$CaCp_2$	1.780	0.063	0.014	0.014	0.001	0.000	0.060	0.060	0.000	0.008
$CaCp^{*+}$	1.752	0.035	0.002	0.001	0.000	0.001	0.101	0.101	0.001	0.014
$CaCp^+$	1.780	0.038	0.000	0.003	0.003	0.085	0.085	0.001	0.008	0.003
$MgCp^*_2$	1.831	0.112	0.007	0.011	0.004	0.003	0.004	0.001	0.002	0.005
$MgCp_2$	1.809	0.138	0.004	0.016	0.016	0.004	0.004	0.001	0.002	0.001
$MgCp^{*+}$	1.796	0.141	0.029	0.028	0.001	0.000	0.003	0.003	0.000	0.000
$MgCp^+$	1.809	0.122	0.031	0.031	0.002	0.000	0.003	0.003	0.000	0.000

3) Intermolecular interactions, agostic interactions.

Table S4. Crystallographic details.

Compound	$MgCp^*_2$	$CaCp^*_2$
Formula	$C_{20}H_{30}Mg$	$C_{20}H_{30}Ca$
Crystal System	Monoclinic	Monoclinic
Space Group	$P2_1/c$	$P2_1/n$
Radiation source	MoKα	Synchrotron
λ (Å)	0.71073	0.41328
a (Å)	9.919(2)	9.6254(3)
b (Å)	12.511(3)	12.2852(4)
c (Å)	22.446(5)	30.7537(9)
β (°)	91.75(3)	96.2650(10)
V (Å^3), Z’	2784.3(10), 1.5	3614.91(19), 2
T (K)	100(1)	12(1)
$(\sin\theta/\lambda)_{max}$ (Å^{-1})	0.71	0.71
Completeness (%)	99.9	99.9
R_{int}	0.0448	0.0551
Mean I/sigma	11.0	45.7
No. of reflections measured	76613	136591
No. of unique reflections	8479	11048
No. of observed reflections (I > 2σ(I)), parameters	8102, 301	9754, 493
$R(F^2)$, $wR(F^2)$	0.054, 0.140	0.026, 0.073
$\Delta\rho_{min}$, $\Delta\rho_{max}$(e Å^{-3})	-0.25, 0.47	-0.24, 0.54
GooF	1.147	1.032
CCDC entry no.	1532483	1532482

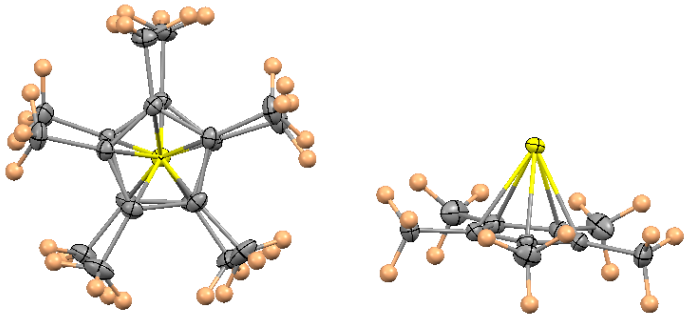

Figure S8. Asymmetric unit of $MgCp^*_2$, Z'=1.5 (with 50% probability ellipsoids). The complete molecule is present in the eclipsed geometry, while for the second molecule, only half of it is present in the asymmetric unit with the central Mg^{2+} ion sitting in the inversion center, resulting in a staggered conformation.

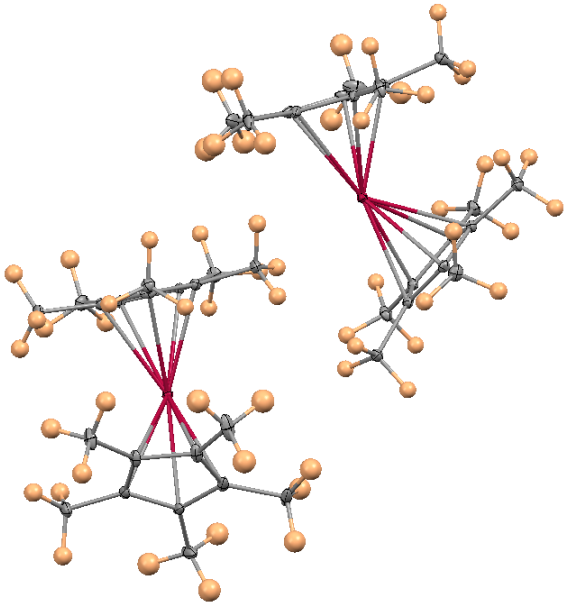

Figure S9. Asymmetric unit of $CaCp^*_2$, Z'=2 (with 50% probability ellipsoids). Both the molecules are in staggered orientations. Only the major disorder components are shown here. Details about the disorder can be found in the CIF and in the residual density plots of Figure S14.

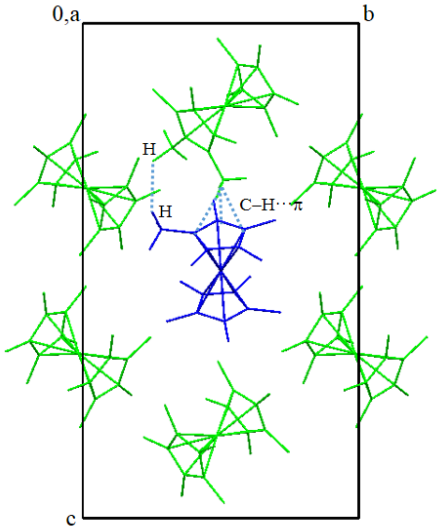

Figure S10. MgCp*$_2$ packing, viewed along *a* axis. One staggered molecule is surrounded by six eclipsed molecules and stabilized via C–H···π and H···H contacts.

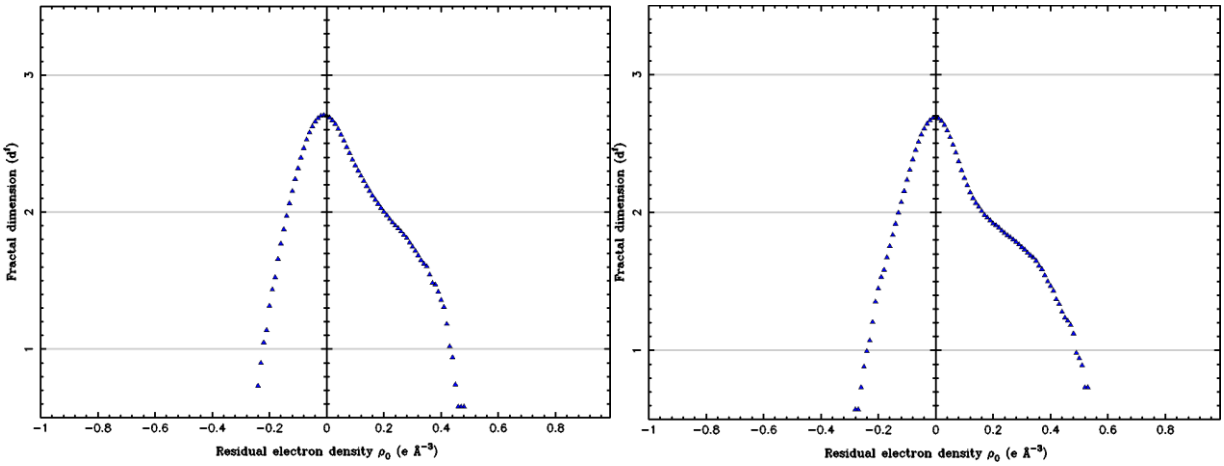

(a) MgCp*$_2$ (b) CaCp*$_2$

Figure S11. Fractal dimension – residual density plots according to Henn and Meindl. The shoulder on the side of the positive residual electron density is caused by neglect of bonding electron density in the Independent Atom Model (IAM). See Figures S12-14.

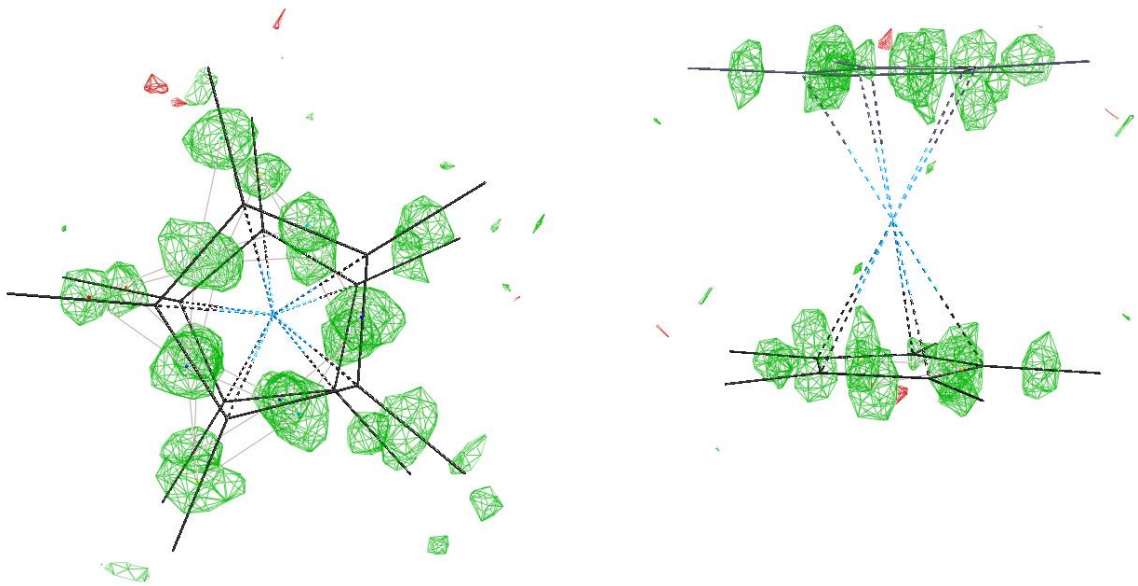

Figure S12. Residual electron density in the asymmetric unit of the $MgCp^*_2$ crystal structure (second molecule completed) at an isovalue of $\pm$ 0.15 eÅ^{-3}. Hydrogen atoms omitted for clarity.

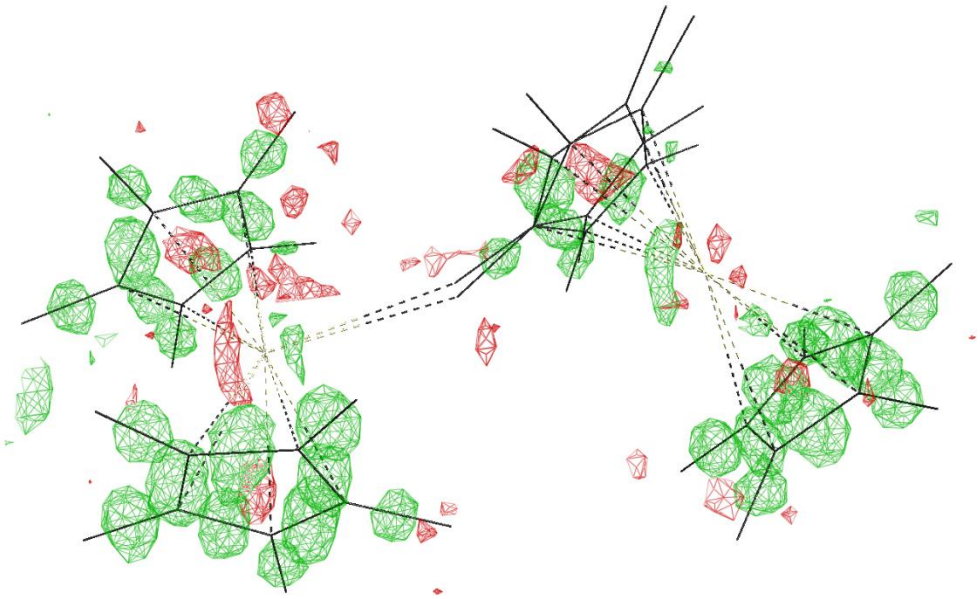

Figure S13. Residual electron density in the asymmetric unit of the $CaCp^*_2$ crystal structure at an isovalue of $\pm$ 0.15 eÅ^{-3}. Hydrogen atoms omitted for clarity.

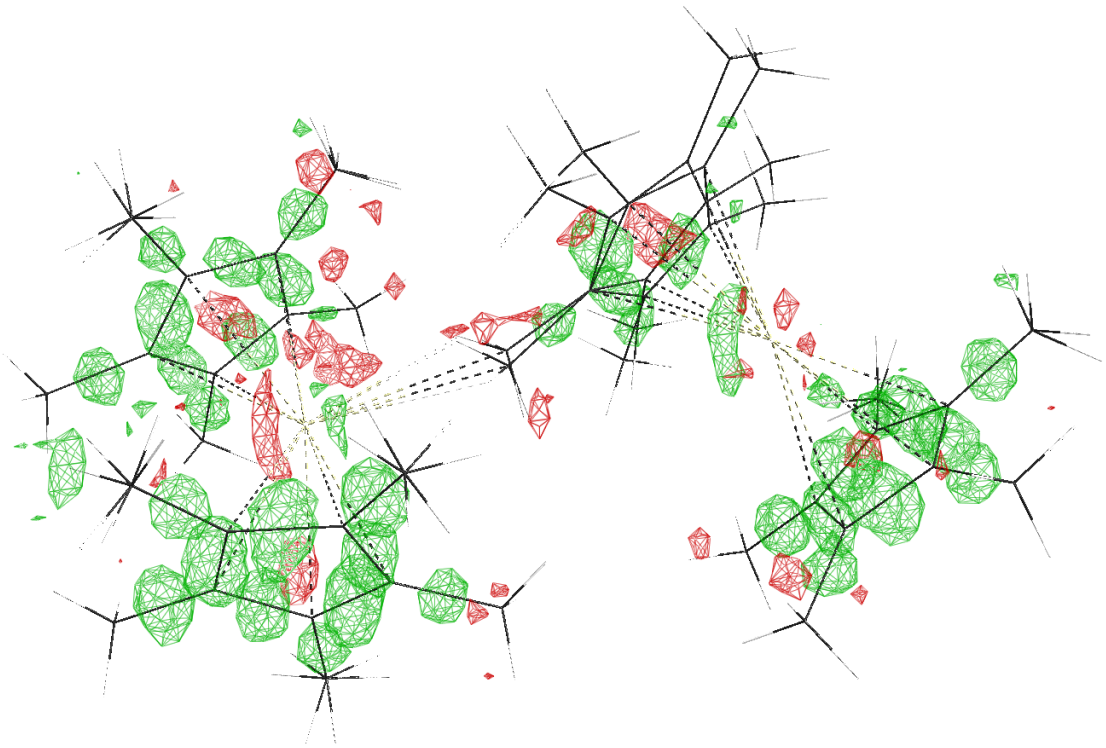

Figure S14. Residual electron density in the asymmetric unit of the $CaCp^*_2$ crystal structure at an isovalue of $\pm$ 0.15 eÅ^{-3}. Full disorder model shown.

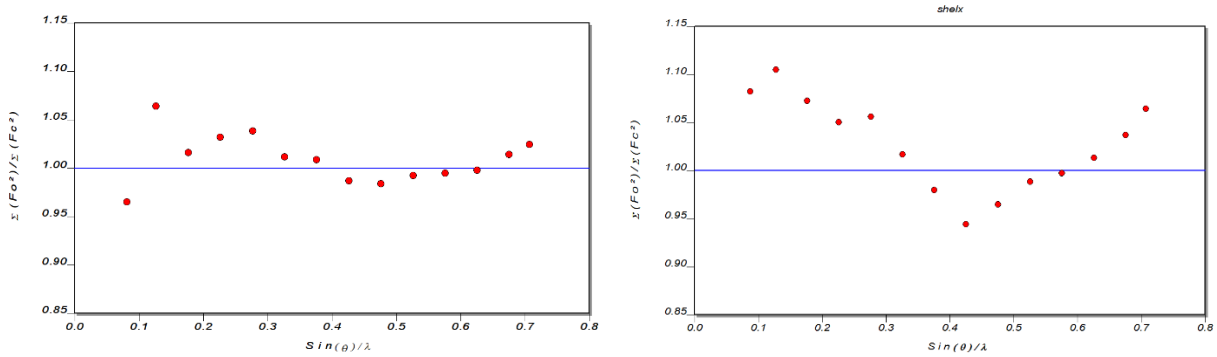

(a) $MgCp^*_2$ (b) $CaCp^*_2$

Figure S15. Binned structure factor ratio over resolution plot for the IAMs. (Sometimes called DRK-plot.)

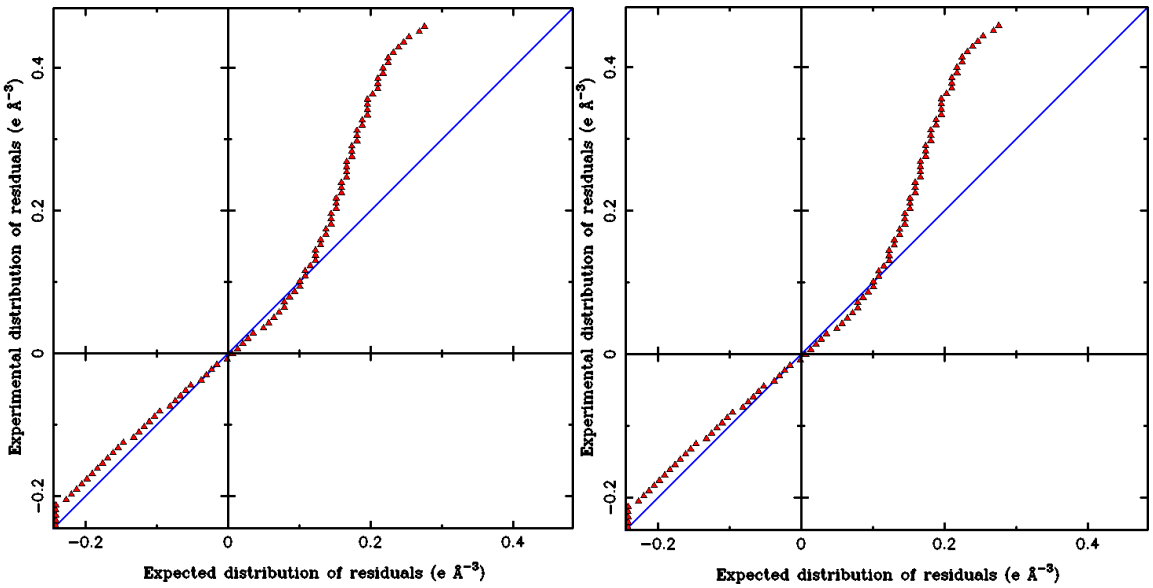

(a) $MgCp^*_2$ (b) $CaCp^*_2$

Figure S16. Normal probability plots for the IAMs.

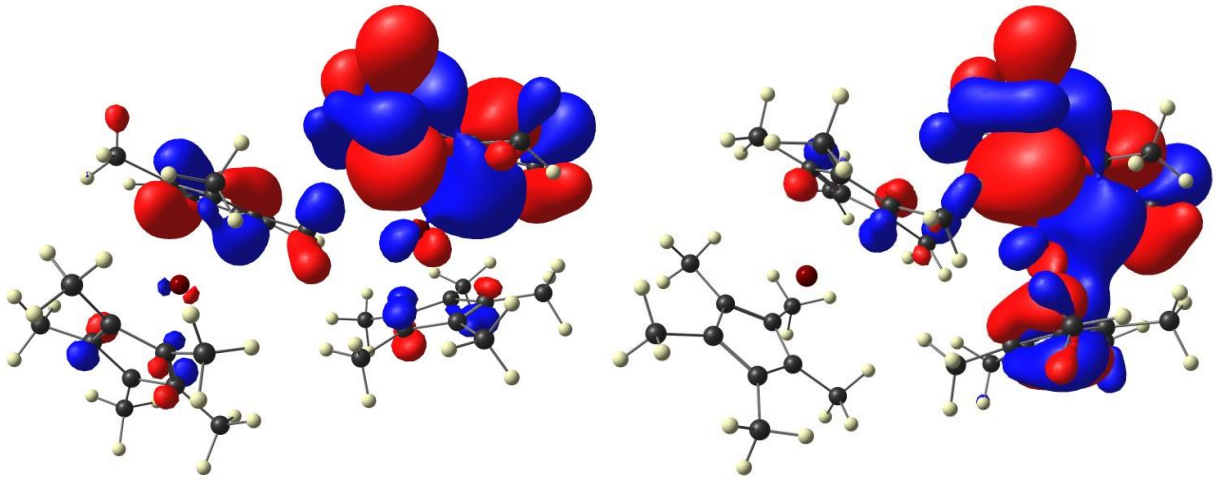

(a) (b)

Figure S17. Salient molecular orbitals in $CaCp^*_2$ dimers (a) HOMO-1 of dimer 1 and (b) HOMO-1 of dimer 2, at a 0.012 au contour value. Color code: blue positive and red negative isosurface.

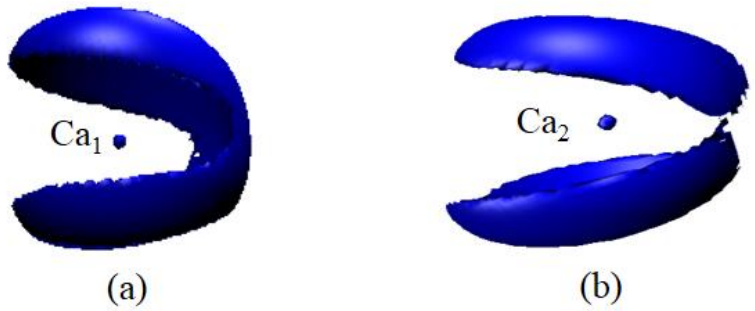

Figure S18. (a) and (b) ELI localization domains around the Ca^{2+} ion (isovalue ELI=1.598) from a calculation of dimer 2 on the geometry as extracted from the crystal structures. In (a), the Ca^{2+} ion is not involved in any C-H…Ca intermolecular interactions, whereas in (b) it is. Compare to Figures 8 (c) and (d) in the main text.

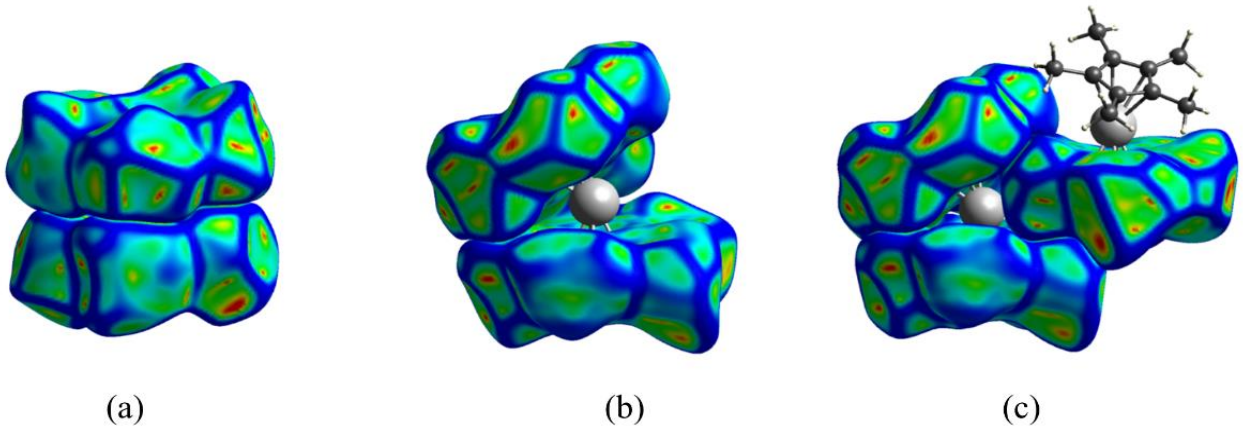

Figure S19. Ligand Hirshfeld surfaces with curvedness mapped onto them for (a) $MgCp^*_2$, (b) $CaCp^*_2$, (c) dimeric unit in $CaCp^*_2$.

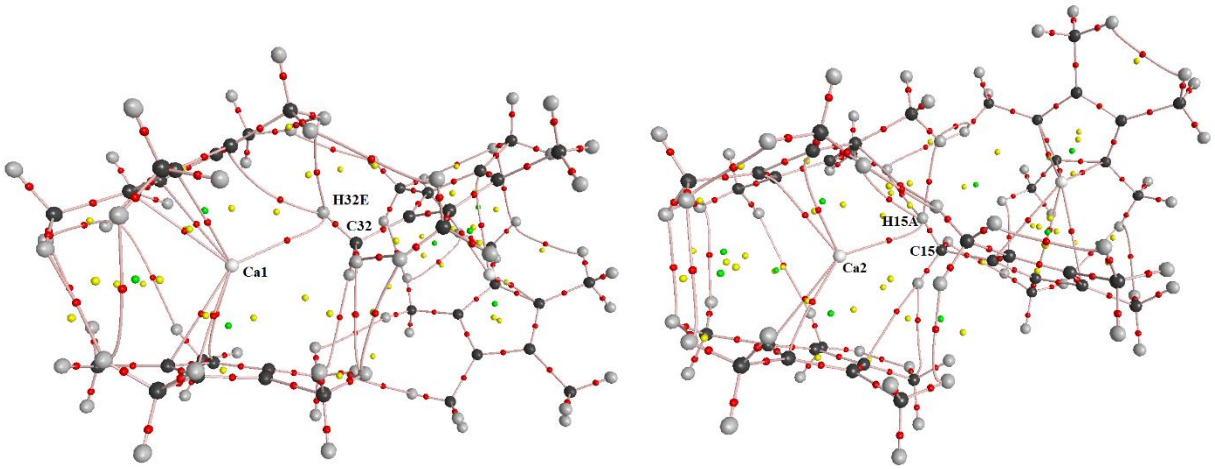

(a) dimer1 (b) dimer2

Figure S20. Topological QTAIM molecular graphs of (a) dimer1 and (b) dimer2. Bond paths and critical points are plotted. Red = bond critical points, yellow = ring critical points, green = cage critical points. The two bond paths found for C-H…Ca pseudo-pregostic interactions are marked with atomic labels.

Table S5. Experimental geometrical parameters of the closest intermolecular C–H⋯Ca interactions and topological electron density parameters for corresponding C-H…Ca bond critical points from theoretical calculations at the experimental geometries of dimer1 and dimer2.

			C–H	H⋯Ca	C⋯Ca	∠ C–H⋯Ca (°)	∠ C_r–C_{Me}⋯Ca (°)
Dimer1	C32-H32E⋯Ca1	d/Å	1.077	2.52(1)	2.951(6)	102.8(6)	163.3(3)
		ρ(r)/eÅ^{-3}		0.08			
		$\nabla^2\rho(r)$/ eÅ^{-5}		1.3			
	C32-H32F⋯Ca1	d	1.077	2.80(1)	2.951(6)	87.2(6)	163.3(3)
		ρ(r)		N/A			
		$\nabla^2\rho(r)$		N/A			
Dimer2	C11-H11B⋯Ca2	d	1.077	2.53(1)	3.022(8)	106.6(8)	113.7(1)
		ρ(r)		N/A			
		$\nabla^2\rho(r)$		N/A			
	C11-H11A⋯Ca2	d	1.077	2.61(1)	3.022(8)	101.6(8)	113.7(1)
		ρ(r)		N/A			
		$\nabla^2\rho(r)$		N/A			
	C15-H15A⋯Ca2	d	1.077	2.87(1)	3.228(1)	99.6(1)	108.2(1)
		ρ(r)		0.08			
		$\nabla^2\rho(r)$		1.3			
	C15-H15C⋯Ca2	d	1.077	2.70(1)	3.228(1)	109.9(1)	108.2(1)
		ρ(r)		N/A			
		$\nabla^2\rho(r)$		N/A			

Table S6. NBO analysis of metal – ligand interactions in dimer 1 and dimer 2. Occupancies in e, orbital energies in a.u., E2 energies in kcal mol^{-1}

$\sigma_{C-H} \rightarrow LV_{Ca\#}$	Occupancy of donor, σ_{C-H}	Energy of donor, σ_{C-H}	E2
Dimer 1			
$\sigma_{C32-H32E}$	1.975	-0.49	1.96
$\sigma_{C32-H32D}$	1.979	-0.48	1.65
$\sigma_{C32-H32F}$	1.980	-0.50	1.48
Dimer 2			
$\sigma_{C11-H11A}$	1.974	-0.49	2.07
$\sigma_{C11-H11B}$	1.979	-0.50	2.09
$\sigma_{C11-H11C}$	1.983	-0.49	0.59
σ_{C1-C11}	1.983	-0.54	0.98
σ_{C1-C5}	1.957	-0.59	2.12
$\sigma_{C15-H15A}$	1.975	-0.49	1.94
$\sigma_{C15-H15C}$	1.980	-0.49	1.86
$\sigma_{C15-H15B}$	1.985	-0.48	0.37
σ_{C5-C15}	1.978	-0.54	0.94
σ_{C5-C4}	1.958	-0.55	2.34

[#] In dimer 1, occupancy/orbital energy of LV_{Ca1} is 0.086e/0.08 a.u.; in dimer 2, occupancy/ orbital energy of LV_{Ca2} is 0.098 e/ 0.12 a.u.

Tables S7. Optimized geometries. Cartesian coordinates in Å.

1) Cp^- [(B3LYP-D /6-311++g(2d,2p)] with D = GD3

6	-1.019021000	-0.637397000	-0.000115000
6	0.291310000	-1.166064000	-0.000178000
6	1.199052000	-0.083302000	-0.000005000
6	0.449759000	1.114575000	0.000187000
6	-0.921103000	0.772170000	0.000110000
1	2.279228000	-0.158241000	-0.000007000
1	0.553793000	-2.216556000	-0.000334000
1	-1.937022000	-1.211594000	-0.000215000
1	-1.750877000	1.467794000	0.000206000
1	0.854897000	2.118704000	0.000358000

2) Cp^{*-} [(B3LYP-D /6-311++g(2d,2p)]

6	-1.197065000	0.128193000	-0.015503000
6	-0.491804000	-1.099549000	-0.015195000
6	0.893152000	-0.807460000	-0.014147000
6	1.043687000	0.600632000	-0.013920000
6	-0.248486000	1.179371000	-0.014775000
6	-2.690284000	0.283773000	0.011197000
6	-1.114258000	-2.466189000	0.007099000
6	2.016594000	-1.803686000	0.009667000
6	2.351939000	1.337536000	0.009203000
6	-0.563868000	2.647790000	0.007351000
1	-3.195951000	-0.523076000	-0.530915000
1	-3.116546000	0.281884000	1.027419000
1	-3.010113000	1.223385000	-0.451103000
1	-0.448594000	-3.223164000	-0.419163000
1	-1.371805000	-2.817330000	1.019085000
1	-2.044075000	-2.502286000	-0.571914000
1	2.402860000	-2.009573000	1.020835000
1	1.712602000	-2.770050000	-0.404204000
1	2.876839000	-1.464958000	-0.579148000
1	2.254912000	2.350967000	-0.392235000
1	2.779711000	1.446109000	1.018797000
1	3.118017000	0.832652000	-0.590806000
1	-1.479426000	2.877931000	-0.548672000
1	-0.712252000	3.052712000	1.021122000
1	0.236189000	3.242330000	-0.444954000

3) MgCp+ [(B3LYP-D /6-311++g(2d,2p)]

12	-0.002346000	-0.004373000	1.389861000
6	-1.127748000	-0.449421000	-0.472142000
6	-0.776765000	0.935288000	-0.468064000
6	0.648662000	1.029449000	-0.465670000
6	1.178885000	-0.296970000	-0.468226000
6	0.080950000	-1.210940000	-0.472843000
1	-1.465429000	1.762532000	-0.516589000
1	-2.127147000	-0.848700000	-0.524480000
1	0.151989000	-2.284756000	-0.526042000
1	2.222282000	-0.561208000	-0.517297000
1	1.222561000	1.940166000	-0.512253000

4) $MgCp^{*+}$ [(B3LYP-D /6-311++g(2d,2p)]

12	0.000929000	0.000588000	1.694231000
6	-0.995203000	-0.716044000	-0.149667000
6	-0.988516000	0.724766000	-0.149804000
6	0.383821000	1.163787000	-0.150110000
6	1.225430000	-0.005866000	-0.150078000
6	0.373050000	-1.167467000	-0.149747000
6	-2.205975000	-1.586875000	-0.330542000
6	-2.190858000	1.607448000	-0.330820000
6	0.851831000	2.579960000	-0.331625000
6	2.717005000	-0.012782000	-0.330846000
6	0.827516000	-2.588027000	-0.331386000
1	-2.406878000	-1.732044000	-1.394001000
1	-2.070476000	-2.573688000	0.108125000
1	-3.098572000	-1.144084000	0.107366000
1	-2.391403000	1.752840000	-1.394327000
1	-3.087830000	1.174882000	0.108466000
1	-2.044840000	2.593674000	0.105756000
1	0.927709000	2.815546000	-1.395150000
1	0.163343000	3.299339000	0.107854000
1	1.835031000	2.745732000	0.104723000
1	2.965007000	-0.012536000	-1.394259000
1	3.187578000	0.864770000	0.108524000
1	3.178937000	-0.896161000	0.106097000
1	0.902816000	-2.823672000	-1.394987000
1	1.808351000	-2.764048000	0.106266000
1	0.131477000	-3.301017000	0.106527000

5) $MgCp_2$ [(B3LYP-D /6-311++g(2d,2p)]

12	-0.000002000	0.000018000	-0.000009000
6	-2.000159000	1.100473000	0.495300000
6	-2.000185000	0.811158000	-0.893543000
6	-2.000250000	-0.599124000	-1.047523000
6	-2.000347000	-1.181402000	0.246108000
6	-2.000259000	-0.130987000	1.199619000
6	2.000268000	0.599371000	1.047375000
6	2.000180000	-0.810928000	0.893737000
6	2.000172000	-1.100607000	-0.495013000
6	2.000257000	0.130672000	-1.199645000
6	2.000324000	1.181344000	-0.246402000
1	2.005470000	-2.083213000	-0.937048000

1	2.005624000	-1.534881000	1.691715000
1	2.005543000	1.134517000	1.982526000
1	2.005629000	2.236081000	-0.466378000
1	2.005767000	0.247341000	-2.270762000
1	-2.005511000	-1.134030000	-1.982807000
1	-2.005619000	1.535332000	-1.691326000
1	-2.005447000	2.082954000	0.937594000
1	-2.005770000	-0.247942000	2.270710000
1	-2.005673000	-2.236192000	0.465811000

6) $MgCp^*_2$ [(B3LYP-D /6-311++g(2d,2p)]

12	0.000002000	-0.000258000	-0.000398000
6	-2.003745000	-0.928688000	-0.782007000
6	-2.003007000	-1.031065000	0.642084000
6	-2.002497000	0.291696000	1.179483000
6	-2.002698000	1.211584000	0.087620000
6	-2.003679000	0.457336000	-1.124619000
6	2.002863000	-0.295196000	-1.178563000
6	2.002967000	1.029173000	-0.645119000
6	2.003346000	0.931057000	0.779268000
6	2.003495000	-0.453919000	1.126034000
6	2.002962000	-1.211813000	-0.083928000
6	-2.110246000	-2.076454000	-1.748895000
6	-2.109119000	-2.305571000	1.434478000
6	-2.108008000	0.651880000	2.636542000
6	-2.108423000	2.708526000	0.194891000
6	-2.110379000	1.022243000	-2.515072000
6	2.108883000	-0.659734000	-2.634501000
6	2.109111000	2.301307000	-1.441319000
6	2.109237000	2.081718000	1.742769000
6	2.109865000	-1.014649000	2.518200000
6	2.109072000	-2.709042000	-0.186735000
1	-3.154628000	-2.328438000	-1.956446000
1	-1.643630000	-1.848270000	-2.707565000
1	-1.637301000	-2.980614000	-1.364598000
1	-3.153448000	-2.583281000	1.606340000
1	-1.638968000	-3.145709000	0.922649000
1	-1.639785000	-2.218080000	2.414677000
1	-3.152316000	0.728511000	2.954120000
1	-1.636887000	-0.093566000	3.277780000
1	-1.639865000	1.611883000	2.855836000

1	-3.152738000	3.034449000	0.217528000
1	-1.639154000	3.088179000	1.102933000
1	-1.638190000	3.213099000	-0.649553000
1	-3.154836000	1.147140000	-2.816371000
1	-1.638745000	2.001919000	-2.596131000
1	-1.642932000	0.374183000	-3.256882000
1	3.153302000	-0.737666000	-2.951405000
1	1.640486000	-1.620204000	-2.851198000
1	1.638304000	0.084000000	-3.278123000
1	3.153451000	2.578494000	-1.613960000
1	1.639821000	2.210910000	-2.421276000
1	1.638953000	3.142979000	-0.932026000
1	3.153484000	2.334644000	1.949851000
1	1.636097000	2.984579000	1.355691000
1	1.642443000	1.856208000	2.701984000
1	3.154253000	-1.138380000	2.820215000
1	1.641989000	-0.364511000	3.257914000
1	1.638461000	-1.994207000	2.601990000
1	3.153471000	-3.034784000	-0.208081000
1	1.638670000	-3.211238000	0.659028000
1	1.640197000	-3.091458000	-1.093821000

7) $CaCp^+$ [(B3LYP-D /6-311++g(2d,2p)]

20	1.412548000	-0.000071000	0.000001000
6	-0.800011000	1.179902000	0.250828000
6	-0.800182000	0.603207000	-1.044465000
6	-0.800331000	-0.807015000	-0.896414000
6	-0.800197000	-1.101930000	0.490514000
6	-0.800273000	0.126048000	1.199532000
1	-0.849174000	-1.528144000	-1.697405000
1	-0.848842000	1.142140000	-1.977822000
1	-0.848710000	2.234127000	0.474955000
1	-0.849203000	0.238560000	2.271423000
1	-0.849063000	-2.086541000	0.928855000

8) $CaCp^{*+}$ [(B3LYP-D /6-311++g(2d,2p)]

20	-0.001740000	0.000805000	1.779923000
6	1.185354000	-0.255493000	-0.404375000
6	0.123327000	-1.206435000	-0.404841000
6	-1.109457000	-0.490258000	-0.405723000
6	-0.809183000	0.903522000	-0.406081000
6	0.609141000	1.048497000	-0.405283000

6	2.652583000	-0.571166000	-0.505824000
6	0.277965000	-2.699330000	-0.506360000
6	-2.482024000	-1.097269000	-0.508299000
6	-1.810476000	2.021584000	-0.507590000
6	1.365598000	2.344767000	-0.507419000
1	2.959800000	-0.637391000	-1.551858000
1	2.903580000	-1.526366000	-0.044756000
1	3.273959000	0.196650000	-0.045105000
1	0.321183000	-3.010834000	-1.552307000
1	-0.557019000	-3.234448000	-0.054343000
1	1.195532000	-3.053482000	-0.036411000
1	-2.770408000	-1.220700000	-1.554474000
1	-3.246527000	-0.474148000	-0.044354000
1	-2.532653000	-2.085285000	-0.050929000
1	-2.022870000	2.253676000	-1.553475000
1	-1.450094000	2.942499000	-0.049360000
1	-2.763520000	1.767592000	-0.043638000
1	1.546406000	2.602543000	-1.553229000
1	2.341789000	2.294015000	-0.024769000
1	0.818676000	3.179063000	-0.068679000

9) $CaCp_2$, linear [(B3LYP-D /6-311++g(2d,2p)]

20	0.000000000	0.001088000	-0.000821000
6	2.348130000	0.033016000	1.204059000
6	2.347826000	-1.134900000	0.403937000
6	2.348728000	-0.734844000	-0.954070000
6	2.349556000	0.680328000	-0.993243000
6	2.349193000	1.154893000	0.340564000
6	-2.348746000	0.733142000	0.955370000
6	-2.349532000	1.134744000	-0.402186000
6	-2.349169000	-0.032270000	-1.203633000
6	-2.348128000	-1.155121000	-0.341405000
6	-2.347860000	-0.682069000	0.992931000
1	2.378855000	-2.150847000	0.765406000
1	2.379416000	0.062835000	2.281964000
1	2.381467000	2.189238000	0.645289000
1	2.382220000	1.289744000	-1.882797000
1	2.380632000	-1.392562000	-1.808552000
1	-2.378919000	-1.292533000	1.881821000
1	-2.380664000	1.389849000	1.810629000
1	-2.382176000	2.151064000	-0.762473000
1	-2.381438000	-0.060909000	-2.281542000
1	-2.379394000	-2.189158000	-0.647270000

10) $CaCp^*_2$, linear [B3LYP/6-311++g(2d,2p)]

20	-0.000054000	0.000030000	-0.000495000
6	2.347617000	0.914649000	0.795192000
6	2.347998000	-0.472735000	1.115075000
6	2.348005000	-1.205536000	-0.105343000
6	2.348701000	-0.271502000	-1.179552000
6	2.348262000	1.038942000	-0.623077000
6	-2.348252000	1.205472000	0.105617000
6	-2.348555000	0.472894000	-1.114977000
6	-2.347736000	-0.914444000	-0.795184000
6	-2.347884000	-1.039030000	0.623026000
6	-2.348555000	0.271356000	1.179613000
6	2.462863000	2.047734000	1.780862000
6	2.464325000	-1.061059000	2.496509000
6	2.465222000	-2.701592000	-0.236189000
6	2.466414000	-0.609957000	-2.642401000
6	2.464919000	2.326001000	-1.396709000
6	-2.465800000	2.701488000	0.237263000
6	-2.464900000	1.061391000	-2.496428000
6	-2.463211000	-2.047493000	-1.780816000
6	-2.464244000	-2.326440000	1.396169000
6	-2.465261000	0.609835000	2.642534000
1	3.508557000	2.291300000	1.993897000
1	1.996865000	1.810404000	2.738505000
1	1.998456000	2.963786000	1.412444000
1	3.510296000	-1.195911000	2.789671000
1	1.991940000	-2.042062000	2.568084000
1	2.007377000	-0.424765000	3.255884000
1	3.511492000	-3.022512000	-0.260567000
1	2.004205000	-3.072990000	-1.152690000
1	1.997786000	-3.226816000	0.598168000
1	3.512672000	-0.684411000	-2.955441000
1	2.003423000	0.145097000	-3.279526000
1	2.000428000	-1.566758000	-2.882883000
1	3.510922000	2.600807000	-1.565606000
1	2.002857000	3.164796000	-0.873931000
1	1.997512000	2.259605000	-2.380394000
1	-3.512106000	3.022026000	0.264514000
1	-2.000726000	3.227294000	-0.598035000
1	-2.002463000	3.072530000	1.152747000
1	-3.510890000	1.190360000	-2.792179000

1	-2.002422000	0.428477000	-3.255332000
1	-1.998024000	2.045121000	-2.565971000
1	-3.508958000	-2.292495000	-1.991939000
1	-1.996898000	-2.963022000	-1.413529000
1	-1.999408000	-1.809113000	-2.739233000
1	-3.510147000	-2.604987000	1.559387000
1	-2.002267000	-2.257990000	2.382236000
1	-1.996314000	-3.163834000	0.876205000
1	-3.511298000	0.689963000	2.954816000
1	-1.994315000	1.563947000	2.884166000
1	-2.007051000	-0.148297000	3.279332000

11) $CaCp^*_2$, bent [(B3LYP-D /6-311++g(2d,2p)]

20	0.000005000	-0.000067000	-0.452871000
6	2.117189000	0.997180000	0.714018000
6	2.013981000	-0.341193000	1.180748000
6	2.256676000	-1.210214000	0.082366000
6	2.513493000	-0.408998000	-1.064553000
6	2.426219000	0.956388000	-0.673454000
6	-2.256146000	1.210162000	0.084460000
6	-2.513331000	0.411011000	-1.063806000
6	-2.426613000	-0.955080000	-0.675038000
6	-2.117571000	-0.998367000	0.712357000
6	-2.013792000	0.339176000	1.181353000
6	1.998926000	2.239539000	1.554051000
6	1.774083000	-0.768939000	2.601787000
6	2.313596000	-2.712008000	0.150125000
6	2.915158000	-0.913025000	-2.424654000
6	2.715556000	2.146976000	-1.547170000
6	-2.312441000	2.711866000	0.154724000
6	-2.914909000	0.917463000	-2.423025000
6	-2.716512000	-2.144004000	-1.550836000
6	-1.999693000	-2.242168000	1.550323000
6	-1.773823000	0.764407000	2.603134000
1	2.966834000	2.547088000	1.960582000
1	1.329371000	2.093818000	2.402213000
1	1.614572000	3.084640000	0.980584000
1	2.713671000	-0.943340000	3.134104000
1	1.201436000	-1.696114000	2.657590000
1	1.222873000	-0.015055000	3.163061000
1	3.307686000	-3.067086000	0.437513000

1	2.079099000	-3.173705000	-0.810096000
1	1.611518000	-3.112461000	0.883304000
1	4.001581000	-1.004040000	-2.516343000
1	2.588819000	-0.244647000	-3.223530000
1	2.498657000	-1.899286000	-2.634787000
1	3.770769000	2.432845000	-1.503389000
1	2.140484000	3.024524000	-1.247100000
1	2.487220000	1.950728000	-2.595976000
1	-3.306431000	3.066885000	0.442535000
1	-2.077592000	3.175039000	-0.804698000
1	-1.610318000	3.110796000	0.888682000
1	-4.001319000	1.008821000	-2.514547000
1	-2.588704000	0.250397000	-3.223051000
1	-2.498244000	1.904012000	-2.631478000
1	-3.771985000	-2.429059000	-1.508037000
1	-2.142315000	-3.022501000	-1.251896000
1	-2.487505000	-1.946265000	-2.599220000
1	-2.967475000	-2.549355000	1.957428000
1	-1.329064000	-2.098473000	2.397991000
1	-1.616843000	-3.086759000	0.975104000
1	-2.713388000	0.938467000	3.135600000
1	-1.200638000	1.691147000	2.660570000
1	-1.223148000	0.009261000	3.163235000

12) CaCp*2, bent [(B3LYP-D /6-311++g(2d,2p)], with D = GD3BJ

20	0.000001	0.000042	-0.444463
6	2.110862	0.992411	0.720781
6	2.011952	-0.348230	1.179150
6	2.251397	-1.209176	0.074878
6	2.501683	-0.400550	-1.067160
6	2.413989	0.961145	-0.667188
6	-2.250997	1.209116	0.076978
6	-2.501562	0.402530	-1.066431
6	-2.414305	-0.959879	-0.668791
6	-2.111158	-0.993621	0.719116
6	-2.011803	0.346208	1.179767
6	1.989894	2.227286	1.567431
6	1.776383	-0.783040	2.596411
6	2.304924	-2.709443	0.129398
6	2.887527	-0.895458	-2.432774
6	2.686807	2.156666	-1.535691
6	-2.304011	2.709309	0.134016
6	-2.887334	0.899846	-2.431187

6	-2.687559	-2.153783	-1.539383
6	-1.990481	-2.229956	1.563683
6	-1.776179	0.778517	2.597785
1	2.958772	2.541638	1.966239
1	1.331409	2.070452	2.421885
1	1.593384	3.072689	1.002966
1	2.717289	-0.942159	3.131067
1	1.221017	-1.720482	2.649105
1	1.211998	-0.039801	3.158669
1	3.302890	-3.070501	0.394792
1	2.052026	-3.162937	-0.830032
1	1.616320	-3.113866	0.872699
1	3.972382	-0.990978	-2.536632
1	2.557244	-0.219671	-3.223589
1	2.465429	-1.878639	-2.645686
1	3.740348	2.449573	-1.501679
1	2.110069	3.029072	-1.224476
1	2.449769	1.964715	-2.583250
1	-3.301859	3.070270	0.399981
1	-2.050929	3.164291	-0.824658
1	-1.615288	3.112250	0.878009
1	-3.972179	0.995651	-2.534889
1	-2.557118	0.225383	-3.223159
1	-2.465141	1.883352	-2.642411
1	-3.741282	-2.446126	-1.506186
1	-2.111425	-3.027033	-1.229441
1	-2.450090	-1.960234	-2.586554
1	-2.959213	-2.543940	1.963136
1	-1.330825	-2.075172	2.417618
1	-1.595519	-3.074859	0.997390
1	-2.717079	0.937203	3.132580
1	-1.220347	1.715586	2.652136
1	-1.212251	0.034044	3.158871